

**UNIVERSITATEA “BABES-BOLYAI” CLUJ-NAPOCA
FACULTATEA DE CHIMIE SI INGINERIE CHIMICA**

Complex combinations with polifunctional organic acids

Rezumat

Elena Ilyes

Coordonator stiintific:

Acad.Prof.Dr. Ionel

Haiduc

INTRODUCTION:

The aim of this work was the study of complex combination with metals that contain anionic carboxylato ligands and neutral coligands with nitrogen donor atoms.

Are described 12 combinations, characterized with infrared spectroscopy and UV and also by diffraction with X ray on monocristal.

The first part of the thesis is dealing with the most important examples from the literature.

ORIGINAL CONTRIBUTION:

Aiming to obtain neutral coordination networks, and taking advantage of the ability of the alkoxo group to generate binuclear nodes, we decided to employ the mandelic acid (H_2mand), which can act as a dianionic ligand (Chart I). As a spacer we have chosen a very common organic molecule, hexamethylenetetramine (hmt), which is known to be a versatile tecton in crystal engineering.

The crystal structure of **1** has been solved, and consists of a neutral 3-D coordination network

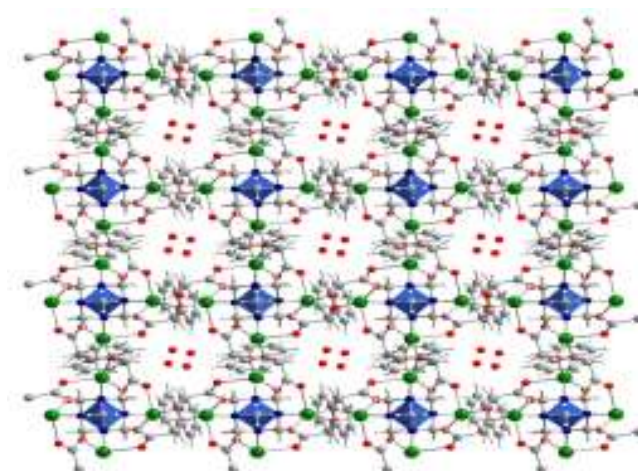


Figure 1. Crystal structure of **1**. View along the channels, which follow the crystallographic *c* axis. The crystallization water molecules hosted into the channels are represented. The hmt molecules are highlighted in blue.

As expected, the neutral alkoxo-bridged binuclear nodes, $\{\text{Cu}_2(\text{mand})_2\}$, are assembled (Figure 2). The copper atoms are crystallographically equivalent. The three-dimensional development of the coordination polymer is quite interesting. First of all, we notice that each carboxylato group is connected through its oxygen atoms to two copper ions: one oxygen atom (O1) chelates together with the alkoxo oxygen (O3) the copper ion, and the other one (O2) is coordinated to the copper ion from another node (*syn-anti* bridging mode). The intranode distance between the copper ions is 3.0017(6) Å. Each copper ion is pentacoordinated, with a slightly distorted square-pyramidal geometry, the apical position being occupied by the oxygen atom arising from the carboxylato group from a neighboring node (Cu1 – O2'' = 2.314(2) Å, '' = 1.25-y, 0.25+x, 0.25-z). The basal plane is formed by one carboxylato and two alkoxo oxygens, and a nitrogen from the hmt ligand (Cu1 – O1 = 1.9500(19); Cu1 – O3 = 1.9351(17); Cu1 – O3' = 1.9616(17); Cu1 – N1 = 2.0514(19) Å; ' = 1-x, 2-y, -z). The hmt molecule acts as a bridge through two out of the four nitrogen atoms, resulting in chains (Figure 3a), which run in perpendicular planes. The connections between the neighbouring perpendicular $\{\text{Cu}_2(\text{hmt})\}$ chains are made by the carboxylato groups (Figures 2, 3b, 3c, 3d). The distance between the copper ions bridged by the carboxylato group is 5.431 Å, while the one between the copper ions connected by the hmt bridge is 5.761 Å.

The most interesting feature of the crystal structure is the presence of channels running along the crystallographic c axis (Figure 1). The crystallization water molecules are hosted into these channels, each one being hydrogen bonded to one carboxylato oxygen atom ($O4W \cdots O2^* = 2.786 \text{ \AA}$; $* = -0.5+x, y, 0.5-z$).

Textural characterization of the metal-organic framework was carried out by measuring the adsorption-desorption isotherms of nitrogen at $-196 \text{ }^\circ\text{C}$, using both micropore and meso- and macropores programs. The surface area was determined using the Langmuir protocol [Langmuir I., *J. Am. Chem. Soc.*, 40, 1631 (1918)], accordingly with the size of the pores of this material and with the composition of the pore walls (quasi homogeneous in polarity), both very close with those exposed by microporous zeolites. Indeed, in the range p/p_0 0 to 0.8, Figure 4 shows a very specific Langmuir isotherm. The surface area determined from this protocol was of $610 \text{ m}^2 \text{ g}^{-1}$. This is smaller than those recently reported for other MOFs [???], but it should be correlated to the complexity of the spacer used in the construction of these materials, and in consequence with the resulted architecture. The pore size was determined using the Horvath-Kawazoe formalism [Horvath G., Kawazoe, K. *J. Chem. Eng. Japan*, 16, 470 (1983)]. This indicated a narrower pore size distribution with a maximum of 7.94 \AA that is in fact very close to that determined from the crystallographic analysis. The pore volume determined from the same calculations corresponded to $0.22 \text{ cm}^3 \text{ g}^{-1}$.

Figure 4. Adsorption isotherm of nitrogen at -196 °C on [Cu₂(mand)₂(hmt)]·

The increase of the p/p_0 ratio from 0.8 to 1.0 was investigated using the meso- and macropore protocol by measuring both the adsorption and desorption isotherms (Figure S1). This indicates an increase of the nitrogen up-take for p/p_0 higher than 0.85. Such a behavior may account for the presence of intercrystalline cages resulted from the agglomeration of the 3 D metal-organic framework units. The pore volume considering the presence of the intercrystalline cages was thus increased to $0.47 \text{ cm}^3 \text{ g}^{-1}$.

The robustness of the crystals was checked by powder XRD at various temperatures (Figure 5). The recorded diffractograms show that the structure of **1** is preserved up to 280 °C. An increase of the crystallinity associated to the loose of the water molecules and solvent occurs till this temperature. Then, after 280 °C a rapid collapse has been evidenced and the metal-organic framework decomposed in CuO

monoclinic phase (JCPDS 48-1548) as it can be deduced from the reflection planes at $2\Theta = 36.6^\circ$, 38.56° and 42.4° .

TGA-DTA experiments confirmed the powder XRD analysis. The thermogravimetric analysis of the structure **1** shows two mass losses, one till around 140°C , associated with an endothermic effect, and the second in the range $280\text{-}360^\circ\text{C}$, associated with an exothermic effect. While the first one could be assigned to the elimination of water, in relation to the XRD analysis, the second loss should correspond to the decomposition of structure **1**.

(Figure 5). Powder XRD diffractograms of **1** in the range $40\text{-}480^\circ\text{C}$.

Figure S2.

In order to test the ability of **1** to host other molecules than water, several chemisorption experiments were carried out. Table 1 shows the uptake and the polarity index of the investigated molecules. Figure 6 shows the evolution of the chemisorptions pulses for hydrogen, toluene, and *p*-xylene. The first pulse corresponds in both cases to the standard. The complete filling of the cages is realized after around 15-20 min for hydrogen and carbon dioxide, and 50-60 min for the aromatic molecules.

The values compiled in Table 1 indicated a different behavior for these molecules. While in the case of carbon dioxide and hydrogen the chemisorption seems to occur via insertion of the molecule inside the metal-organic framework channels, for the aromatic molecules this should occur inside and outside the intercrystalline cages. Table 1 also compiles the polarity, basicity and acidity of these molecules when they

act as solvents.-J. Catalán, in: G. Wypych (Ed.), Handbook of Solvents: Solvent effects based on pure solvent scales, William Andrew, Inc. and ChemTec Publishing, Toronto-New York, 2001. p. 583-616. Water was introduced as a reference molecule. These data shows that the up-take of the aromatic molecules can be correlated with both polarity and basicity. Thus the decrease of the polarity may be associated with self association of these molecules while the increased basicity with the interaction of the mandelic acid incorporated in the framework.

Thermal analysis of the samples exposed to the chemisorptions of aromatic molecules (Figure S2) showed these molecules were removed before 200 °C without any damage of the the metal-organic framework. Once the molecules were removed at 200 °C the structure **1** was able to re-capture the same volume of aromatic molecule as it was proved from three successive cycle

Figure 6 Chemisorption profiles for toluene (a), *p*-xylene (b) and hydrogen (c)

Table 1. Uptake of chemisorption of benzene, toluene, *p*-xylene, carbon dioxide and hydrogen

Chemisorbed molecule	Uptake (cm ³ /g)	Solvent polarity	Solvent basicity	Solvent acidity
Benzene	12.3	0.667	0.124	0.000
Toluene	37.7	0.655	0.128	0.000
<i>p</i> -xylene	74.9	0.617	0.160	0.000
CO ₂	0.23	Non polar		
H ₂	1.6	Non polar		
H ₂ O	-	0.962	0.025	1.062

Figure S2). TGA-DTA curves for structure 1 after chemisorptions

of toluene

As it was mentioned above the behavior of hydrogen and carbon dioxide was different to that of aromatic molecules. They were chemisorbed in volumes very close to that determined from the adsorption of nitrogen. To achieve information about this behavior additional TPD, thermogravimetric and CO₂-DRIFT experiments have been carried out for carbon dioxide. All these measurements showed that the desorption occurs completely before 100 °C, while the degassed material was able to chemisorb another volume of carbon dioxide. CO₂-TPD experiments indicated (Figure S) a desorption of CO₂ corresponding to 0.13-0.17 cm³/g.